Journal of Statistical Physics, Vol. 27, No. 2, 1982

Truncated Navier–Stokes Equations: Continuous Transition from a Five-Mode to a Seven-Mode Model

Laura Tedeschini-Lalli[1]

Received June 12, 1981

A two-parameter family of nonlinear differential equations $\dot{\mathbf{x}} = F(\mathbf{x}, R, \epsilon)$ is studied, which allows one to connect continuously, as ϵ varies from zero to one, the different phenomenologies exhibited by a model of 5-mode truncated Navier–Stokes equations and by a 7-mode one extending it. A critical value is found for ϵ, at which the most significant phenomena of the 5-mode system either vanish or go to infinity. New phenomena arise then, leading to the 7-mode model.

KEY WORDS: Navier–Stokes equations; truncations of the Navier–Stokes equations; stationary bifurcation; Hopf bifurcation; period-doubling bifurcation; bifurcation of a periodic orbit into a two-torus; turbulence; strange attractors.

1. INTRODUCTION

In order to give a mathematical interpretation to the phenomenon of turbulence in fluids, many numerical investigations were performed on models of simple nonlinear equations which, although deterministic, display a chaotic behavior as one or more parameters increase beyond certain critical values. We refer to Ref. 1 for a wide review of studies in this line, while Ref. 2 provides the theoretical framework to understand the different phenomena that occur in such models.

Directly connected with the study of fluid motion are the models obtained by truncating to a finite number of modes the Fourier series expansion of the bidimensional Navier–Stokes equations for an incompressible fluid on a torus. In such a way one obtains a one-parameter

Supported by G.N.F.M., C.N.R.

[1] Istituto Matematico "G. Castelnuovo," Università di Roma, Rome, Italy 10085.

0022-4715/82/0200-0365$03.00/0

family of ordinary differential equations, where the parameter is proportional to the Reynolds number.[3]

Recently two interesting models of this kind were carefully studied, one obtained by a five-mode truncation[4,5] and the other one by a seven-mode extending it.[6] The two models exhibit quite different features concerning the onset of turbulence and the postturbulence behavior. A natural question arises then, which is relevant about any kind of highly truncated models of systems actually having infinitely many degrees of freedom; the question is how truncation affects the phenomenology exhibited by the system. In this work we consider a model which allows one to connect continuously, by means of a parameter ϵ, the two phenomenologies.

Most of our investigations are numerical, and they were performed on a CDC 7600. Numerical integration, throughout this paper, means integration by a Runge–Kutta method of fourth order. We consider periodic solutions as fixed points of the associated Poincaré map; in this way one can fit well-known numerical methods for searching fixed points. We used Newton's method, because it is not affected by the attracting or repulsive nature of the orbit. One can thus "follow" periodic orbits continuously as the parameters change, via an iterative procedure; this is possible because, as it is reasonable to think, small perturbations of the parameters cause small perturbations on the coordinates of a fixed point, provided that it still exists.

A summary of the phenomenologies exhibited by the two models in question can be found in Section 2, together with some remarks about their analogies and differences. Section 3 introduces the connecting model, and the crucial values of ϵ, ϵ_1, and ϵ_3. Sections 4, 5, and 6 are devoted to the detailed study of different phenomena, while Section 7 describes a model of the same kind exhibiting no chaotic behavior.

2. THE FIVE-MODE AND THE SEVEN-MODE MODELS

Since in this work we study the connections between the two models studied in Refs. 4–6, it seems useful to report here a concise summary of the known results about them, referring to these references for details, and introducing some new notations to better connect the two phenomenologies. The two pictures in Fig. 1 can help provide better comprehension.

Truncating the Fourier series expansion on the set $L_5 = \{\mathbf{k}_1 = (1,1), \mathbf{k}_2 = (3,0), \mathbf{k}_3 = (2,-1), \mathbf{k}_4 = (1,2), \mathbf{k}_5 = (0,1)\}$ and taking a force acting on the mode $\mathbf{k}_3$, the bidimensional Navier–

Truncating the Fourier series expansion on the set $L_7 = L_5 \cup \{\mathbf{k}_6 = (1,0), \mathbf{k}_7 = (1,2)\}$ and taking a force acting on the mode $\mathbf{k}_3$ the bidimensional Navier–Stokes equations be-

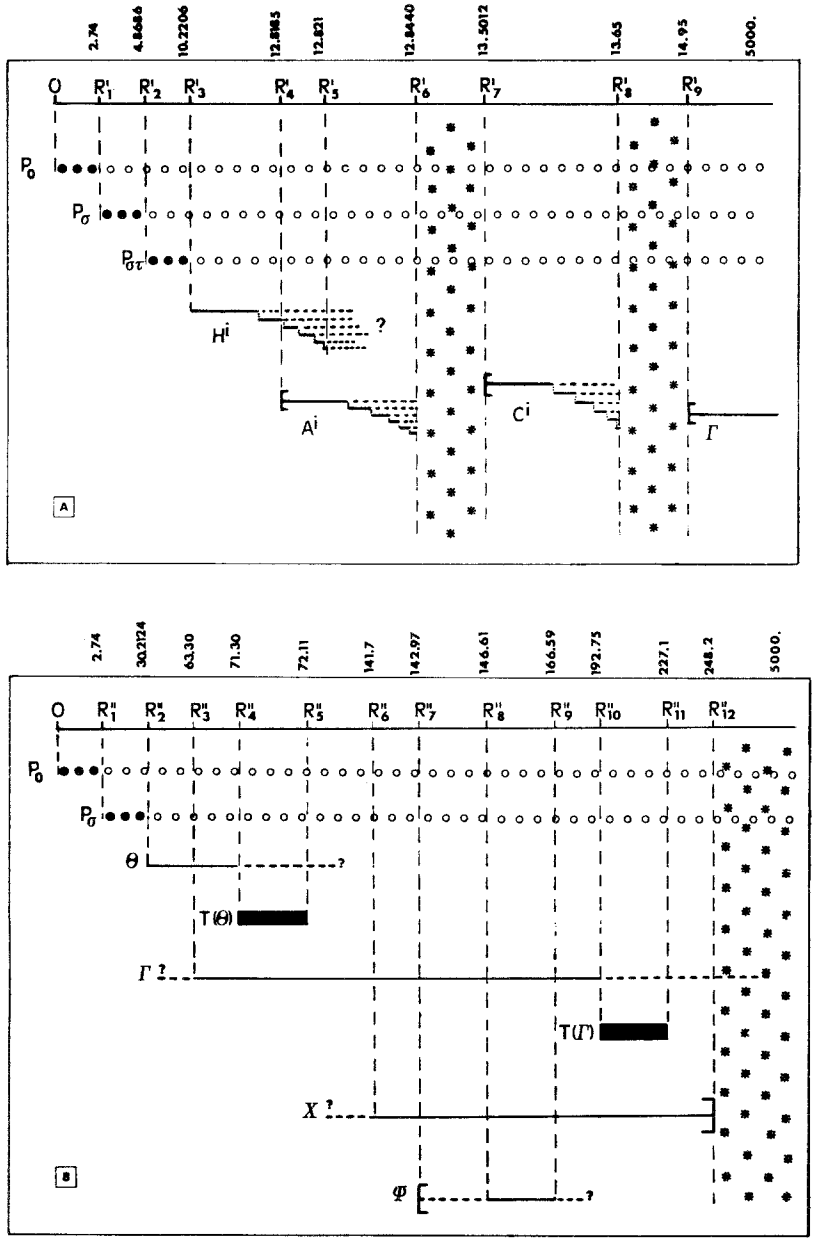

Fig. 1. Graphical summary (not in scale) of the phenomenologies exhibited by system (2.1) (Fig. 1A) and system (2.2) (Fig. 1B), as R varies. A sequence of ●●● indicates for that range of R a stable fixed point, a sequence of ∘ ∘ ∘ an unstable fixed point; a continuous line —— a stable periodic orbit, a broken line - - - an unstable periodic orbit; a black tube ▬▬ an attracting torus T^2; a set of * * * turbulent regime. Symmetrical points, orbits, tori undergoing identical behavior due to the symmetries of the systems are identified.

Stokes equations become

$$\begin{aligned}
\dot{x}_1 &= -2x_1 + 4\sqrt{5}\,x_2x_3 + 4\sqrt{5}\,x_4x_5 \\
\dot{x}_2 &= -9x_2 + 3\sqrt{5}\,x_1x_3 \\
\dot{x}_3 &= -5x_3 - 7\sqrt{5}\,x_1x_2 + R \qquad (2.1) \\
\dot{x}_4 &= -5x_4 - \sqrt{5}\,x_1x_5 \\
\dot{x}_5 &= -x_5 - 3\sqrt{5}\,x_1x_4
\end{aligned}$$

(a) For $0 \leqslant R \leqslant R_1 = \sqrt{7.5}$ there is only one stationary solution, P_0, which is stable and globally attractive.

(b) For $R_1 < R \leqslant R_2' \cong 4.8686$ there are two other stable attracting fixed points P_σ, bifurcated from P_0 at $R = R_1$, as it has become unstable. (σ is the sign of the coordinates x_1, x_2).

(c) For $R_2' < R \leqslant R_3' \cong 10.2206$ there are four more stable attracting fixed points $P_{\sigma\tau}$ (τ is the sign of coordinate x_5); $P_{\sigma+}$ and $P_{\sigma-}$ bifurcate from P_σ at $R = R_2'$ as P_σ becomes unstable.

(d) At $R = R_3'$ four stable symmetric periodic orbits $H_{\sigma\tau}^0$ arise via a direct Hopf bifurcation from $P_{\sigma\tau}$, each around one $P_{\sigma\tau}$, now unstable.

(e) For $R_3' < R \leqslant R_5' \cong 12.821$ four identical sequences $H_{\sigma\tau}^i$ of periodic orbits take place in connection with an infinite sequence of bifurcations. At the ith bifurcation, which occurs at $R = \rho_i$, each orbit $H_{\sigma\tau}^{i-1}$ becomes unstable because a real eigen-

come

$$\begin{aligned}
\dot{x}_1 &= -2x_1 + 4\sqrt{5}\,x_2x_3 + 4\sqrt{5}\,x_4x_5 \\
\dot{x}_2 &= -9x_2 + 3\sqrt{5}\,x_1x_3 \\
\dot{x}_3 &= -5x_3 - 7\sqrt{5}\,x_1x_2 + 9x_1x_7 + R \\
\dot{x}_4 &= -5x_4 - \sqrt{5}\,x_1x_5 \qquad (2.2) \\
\dot{x}_5 &= -x_5 - 3\sqrt{5}\,x_1x_4 + 5x_1x_6 \\
\dot{x}_6 &= -x_6 - 5x_1x_5 \\
\dot{x}_7 &= -5x_7 - 9x_1x_3
\end{aligned}$$

(α) For $0 \leqslant R \leqslant R_1 = \sqrt{7.5}$ there is only one stationary solution, P_0, which is stable and globally attractive.

(β) For $R_1 < R \leqslant R_2'' \cong 30.2124$ there are two other stable attracting fixed points, P_σ, bifurcated from P_0 at $R = R_1$, as it has become unstable. (σ is the sign of the coordinates x_1, x_2, x_7.)

(γ) For $R > R_2''$ the three fixed points of (2.2) are all unstable.

(δ) At $R = R_2''$ two stable symmetric periodic orbits Θ_σ arise via a direct Hopf bifurcation from P_σ, each around one P_σ. The two Θ_σ, which owing to the symmetries of the model undergo identical behavior as R increases, become unstable at $R = R_4'' = 71.30$ because a pair of complex conjugate eigenvalues of the Liapunov matrix of their Poincaré map crosses the unit circle.

(ϵ) For $R_4'' \leqslant R \leqslant R_5'' \cong 72.11$ two attracting 2-tori $T(\Theta_\sigma)$, bifurcated one from each Θ_σ, are present. For $R > R_5''$ they do not attract any more, and they do not seem to bifurcate into any other attractor, since every point randomly chosen in a neighborhood of

value of its Poincaré map crosses the unit circle through -1, bifurcating into the stable periodic orbit $H^i_{\sigma\tau}$, which has doubled period. The sequence $\{\rho_i\}$ of the bifurcation values, is found to be compatible with Feigenbaum's conjecture, namely,

$$\lim_{i\to\infty} \frac{\rho_i - \rho_{i-1}}{\rho_{i+1} - \rho_i} = \delta \cong 4.6692$$

Thus, a value can be estimated, $\rho_\infty \cong 12.821$, at which the sequence of bifurcations accumulates.

(f) At $R = R'_4 \cong 12.8185$ four more symmetric orbits arise, which are stable and attracting, $A^0_{\sigma\tau}$; they have spatial structure different from $H^i_{\sigma\tau}$; in fact each $A^0_{\sigma\tau}$ winds up around two fixed points, namely, $P_{+\tau}$ and $P_{-\tau}$; the sign τ indicates that two of them are contained in the half-space $x_5 < 0$ and the other two in $x_5 > 0$. As R decreases to R'_4 a real eigenvalue of the Liapunov matrix of the Poincaré map tends to join the unit circle at $+1$, and each $A^0_{\sigma\tau}$ coalesces with an unstable orbit $A^*_{\sigma\tau}$ which is present at the same time. As R increases, R'_4 can thus be regarded as a "birth" value of $A^0_{\sigma\tau}$.

(g) For $R'_4 < R < R'_6 \cong 12.8440$ a second sequence of infinite bifurcations gives rise to four identical sequences of periodic orbits $\{A^i_{\sigma\tau}\}$ with the same characteristics of the sequences $\{H^i_{\sigma\tau}\}$. Also the sequence $\{\mu_i\}$ of the bifurcation points for $A^i_{\sigma\tau}$ is found to be compatible with Feigenbaum's conjecture, and $\mu_\infty = 12.8440$ is estimated to be the value of R for which the bifurcations accumulate.

(h) For $R'_6 < R < R'_7 \cong 13.5012$ two symmetric strange attractors are present, one located in the half-space $x_5 < 0$, and the other in $x_5 > 0$.

Θ_σ is attracted by other stable periodic orbits present at the same time.

(ζ) For $63.30 \cong R''_3 < R < R''_{10} \cong 192.75$ two symmetric orbits Γ_τ are present, which are stable and attracting. As R decreases beyond R''_3 a pair of complex conjugate eigenvalues crosses the unit circle, so that Γ_τ already exists, unstable, for $R < R''_3$. Its origin has not been detected. The sign τ indicates that each Γ_τ is contained either in the half-space $x_5 < 0$ or in $x_5 > 0$.

(η) For $R''_{10} < R < R''_{11} \cong 227.1$ two attracting 2-tori $T(\Gamma_\tau)$ arise, each from one Γ_τ, as Γ_τ become unstable at $R = R''_{10}$ because a pair of complex conjugate eigenvalues crosses the unit circle. For $R > R''_{11}$ the tori $T(\Gamma_\tau)$ do not attract any more, and they do not seem to bifurcate into any other attractor.

(ϑ) For $141.7 \cong R''_6 < R < R''_{12} \cong 248.2$ two other symmetric periodic orbits are present, χ_1 and χ_2, which are stable and attracting. As R de-

creases beyond R_6'' a pair of complex conjugate eigenvalues of their Poincaré map crosses the unit circle, so that they already exist, unstable, for $R < R_6''$, but their origin has not been detected. As R increases to R_{12}'' a real eigenvalue tends to join the unit circle at $+1$, and each χ coalesces with an unstable orbit χ^* which is present at the same time. As R increases, R_{12}'' can thus be regarded as a "death" value for χ.

(i) For $R_7' < R < R_8' \cong 13.65$ a third sequence of infinite bifurcations gives rise to four more identical sequences of periodic orbits $\{C_{\sigma\tau}^i\}$, with spatial features and origin similar to those of $\{A_{\sigma\tau}^i\}$. The sequence $\{\nu_i\}$ of the bifurcation points of $\{C_{\sigma\tau}^i\}$ has the same characteristics as the sequences $\{\rho_i\}$ and $\{\mu_i\}$.

(j) For $R_8' < R < R_9' \cong 14.95$ the two symmetric strange attractors that disappeared at $R = R_7'$ because of the birth of stable orbits $C_{\sigma\tau}^0$, are again present.

(k) For $R > R_9'$ any trajectory rapidly becomes periodic, because of two new stable periodic orbits Γ_τ. (τ indicates that one of them is contained in the half-space $x_5 < 0$ and the other in $x_5 > 0$.)

(ι) For $146.61 \cong R_8'' < R < R_9'' = 166.59$ two symmetric orbits are present, ψ_1 and ψ_2, which are stable and attracting. As R decreases beyond R_8'' or increases beyond R_9'', a real eigenvalue of the Poincaré map for ψ actually crosses the unit circle through $+1$. Following ψ for values of $R < R_8''$, a "birth" value $R_7'' \cong 142.97$ was found at which unstable ψ arises with a twice-unstable ψ^*; (we will see in more detail an analogous case in Section 5). No "death" value for ψ has been determined, as R increases.

(κ) For $R > R_{12}''$ no simple attractor is present at such large values of R. Up to the values investigated ($R = 5000$), any randomly chosen initial data yield a completely chaotic trajectory, sensitively dependent on initial conditions.

Remarks. Looking at Fig. 1 one can easily check that both system (2.1) and system (2.2) display cases of hysteresis, i.e., simultaneous occurrence of distinct attractors, not justifiable by the symmetries of the systems.

The onset of turbulence is different in the two systems. In fact in system (2.1) it is connected with infinite sequences of bifurcations of periodic orbits into periodic orbits. Two strange attractors are present,

symmetrically placed with respect to the hyperplane $x_5 = 0$. In system (2.2), instead, turbulence is reached through finite sequences of bifurcations of attractors into attractors of higher dimension, leading to a unique strange attractor at high values of R. The finiteness of these sequences is pointed out in Ref. 6 by affirming that for values of R slightly greater than R_{11}'', R_5'' respectively, any randomly chosen initial data in a neighborhood of the unstable 2-tori $T(\Gamma_\tau)$, $T(\Theta_\sigma)$ is attracted by periodic orbits elsewhere displaced in the phase space.

No sequence of period-doubling bifurcations seems present in system (2.2).

At high values of R system (2.1) displays periodic behavior (the orbit Γ), while system (2.2) exhibits chaos at every value of $R > R_{12}''$ investigated.

3. THE CONNECTING MODEL AND STUDY OF STATIONARY SOLUTIONS

We tried to face the problem of the strong qualitative difference in the asymptotic behavior of the two models described in Section 2, from a perturbative point of view. Let us consider the two-parameter family of ordinary differential equations:

$$\begin{aligned}
\dot{x}_1 &= -2x_1 + 4\sqrt{5}\, x_2x_3 + 4\sqrt{5}\, x_4x_5 \\
\dot{x}_2 &= -9x_2 + 3\sqrt{5}\, x_1x_3 \\
\dot{x}_3 &= -5x_3 - 7\sqrt{5}\, x_1x_2 + 9\epsilon x_1x_7 + R \\
\dot{x}_4 &= -5x_4 - \sqrt{5}\, x_1x_5 \\
\dot{x}_5 &= -x_5 - 3\sqrt{5}\, x_1x_4 + 5\epsilon x_1x_6 \\
\dot{x}_6 &= -x_6 - 5\epsilon x_1x_5 \\
\dot{x}_7 &= -5x_7 - 9\epsilon x_1x_3
\end{aligned} \tag{3.1}$$

For $\epsilon = 1$ the model is the same as (2.2), studied in (6), while for $\epsilon = 0$ the phase space is the direct sum of two spaces, $\mathbb{R}^5 \oplus \mathbb{R}^2$, on which a solution $\mathbf{x}(t)$ has coordinates $x_i(t)$ given by the solution of system (2.1) for $i = 1, \ldots, 5$ and $x_6(t) = x_6(0) \cdot e^{-t}$, $x_7(t) = x_7(0) \cdot e^{-5t}$.

The problem is now to find values of (R, ϵ) critical for the asymptotic behavior of solutions of this system.

We first observe that system (3.1) is invariant under the symmetries

$$(\alpha) \quad (x_1, x_2, x_3, x_4, x_5, x_6, x_7) \longleftrightarrow (x_1, x_2, x_3, -x_4, -x_5, -x_6, x_7)$$

$$(\beta) \quad (x_1, x_2, x_3, x_4, x_5, x_6, x_7) \longleftrightarrow (-x_1, -x_2, x_3, -x_4, x_5, -x_6, -x_7)$$

$$(\gamma) \quad (x_1, x_2, x_3, x_4, x_5, x_6, x_7) \longleftrightarrow (-x_1, -x_2, x_3, x_4, -x_5, x_6, -x_7)$$

which form a group together with the identity transformation.

System (3.1) has the following stationary properties:

For $0 \leqslant R \leqslant R_1 = (7.5)^{1/2}$ and $\forall \epsilon$, the system admits only one stationary solution P_0, with coordinates $x_i = 0$ for $i = 1, 2, 4, \ldots, 7$ and $x_3 = R/5$; P_0, is stable and, by numerical evidence, globally attractive; at $R = R_1$ a real eigenvalue of the Liapunov matrix at P_0 crosses the imaginary axis, and two stable stationary solutions arise, P_+ and P_-, bifurcated from P_0, with coordinates

$$x_1 = \sqrt{6}\, x_2$$

$$x_2 = \sigma 5 \left[\frac{2R - (30)^{1/2}}{2(30)^{1/2}(175 + 243\epsilon^2)} \right]^{1/2}$$

$$x_3 = (3/10)^{1/2}$$

$$x_4 = x_5 = x_6 = 0$$

$$x_7 = -\frac{27\epsilon}{5\sqrt{5}}\, x_2$$

where $\sigma = \pm$; P_+ and P_- are symmetrical and go through identical behavior, so that they will be referred to as P_σ in the following.

If we consider the Liapunov matrix $L_\sigma(R, \epsilon)$ at $P_\sigma(R, \epsilon)$, we have that

(1) $$R = R_s(\epsilon) = \frac{400 - 1632\epsilon^2}{5(30)^{1/2}(3 - 25\epsilon^2)}$$

is the condition on (R, ϵ) to have a real eigenvalue of the matrix vanish, and so $(R_s(\epsilon), \epsilon)$ is a value critical for P_σ, possibly a value for a stationary bifurcation; and

(2) $$R = R_h(\epsilon) = R_1 + \frac{36(175 + 243\epsilon^2)}{25(30)^{1/2}(9 - 5\epsilon^2)}$$

is the condition to have two purely imaginary eigenvalues, so that $(R_h(\epsilon), \epsilon)$ is a value critical for P_σ, possibly a value for a Hopf bifurcation.

Both $R_s(\epsilon)$ and $R_h(\epsilon)$ are increasing functions, with $R_s(0) < R_h(0)$, and $R_s(\epsilon) \to \infty$ as $\epsilon \uparrow \epsilon_3 = \sqrt{3}/5$, while $R_h(\epsilon)$ is finite for every $\epsilon \in [0, 1]$. We determined the value $\epsilon_1 \cong 0.26832$ for which $R_s(\epsilon_1) = R_h(\epsilon_1)$. We have thus a partition of the interval $[0, 1]$ in three intervals $[0, \epsilon_1]$, (ϵ_1, ϵ_3), and $[\epsilon_3, 1]$, characterized by a different behavior of the stationary solutions P_σ as R varies:

(i) $0 \leqslant \epsilon < \epsilon_1$

We have $R_s(\epsilon) < R_h(\epsilon)$, so that fixed ϵ, the P_σ's lose stability at $R = R_s(\epsilon)$ bifurcating into four stable stationary solutions $P_{\sigma\tau}$ (two from each P_σ),

with components

$$x_1 = -\sigma \frac{1}{[a(\epsilon)]^{1/2}}$$

$$x_2 = -\sigma 5\sqrt{5}\, R \frac{[a(\epsilon)]^{1/2}}{b(\epsilon)}$$

$$x_3 = 15R \frac{a(\epsilon)}{b(\epsilon)}$$

$$x_4 = \tau \left\{ \frac{1}{a(\epsilon)} \left[\frac{(x_3)^2}{3} - \frac{1}{10} \right] \right\}^{1/2}$$

$$x_5 = \sigma\sqrt{5}\, [a(\epsilon)]^{1/2} x_4$$

$$x_6 = 5\sqrt{5}\, \epsilon x_4$$

$$x_7 = \sigma 27 \epsilon R \frac{[a(\epsilon)]^{1/2}}{b(\epsilon)}$$

where $\sigma, \tau = \pm 1$ and $a(\epsilon) = 3\text{–}25\epsilon^2$, and $b(\epsilon) = 400\text{–}1632\epsilon^2$. We will refer to these solutions as $P_{\sigma\tau}$ in the following.[2]

(ii) $\epsilon_1 < \epsilon < \epsilon_3$

We have $R_h(\epsilon) < R_s(\epsilon) < +\infty$; fixing ϵ, as R increases, the P_σ's lose stability at $R = R_h(\epsilon)$ generating two symmetric stable periodic orbits Θ_σ via a direct Hopf bifurcation; as R increases further, the now unstable P_σ's bifurcate into four unstable stationary solutions $P_{\sigma\tau}$, at $R = R_s(\epsilon)$.

(iii) $\epsilon_3 < \epsilon \leqslant 1$

Fixing ϵ, P_σ lose their stability at $R = R_h(\epsilon)$ undergoing a Hopf bifurcation. No more stationary bifurcation takes place.

Studying numerically the behavior of the eigenvalues λ_i, with $i = 1, \ldots, 7$ for $L_\sigma(R, \epsilon)$, we found that what actually happens is that five of them in any case have a negative real part. The other two, say λ_1 and λ_2, are complex conjugate numbers, placed in the left half-plane for small R and $\forall\epsilon$. Fixing ϵ and regarding $\lambda_{1,2}$ as complex functions of R, we see that $|\mathrm{Im}[\lambda_{1,2}(R)]|$ is a decreasing function and $\mathrm{Re}[\lambda_{1,2}(R)]$ an increasing one, up to a value of R at which $\mathrm{Im}(\lambda_{1,2})$ vanishes and λ_1 and λ_2 join on the real axis. From this value on, $\lambda_{1,2}(R)$ are real monotone functions, one increasing, the other one decreasing. Such behavior is more understandable by Fig. 2. All of the bifurcations of P_σ are due to one or both of $\lambda_{1,2}(R)$,

[2] The condition on (R, ϵ) to have two purely imaginary eigenvalues for the matrix $L_\sigma(R, \epsilon)$ coincides with the condition for which it has two real eigenvalues symmetric with respect to zero. This is actually the case in this range of ϵ, so that fixing $\epsilon \in [0, \epsilon_1)$ no Hopf bifurcation takes place for the P_σ's.

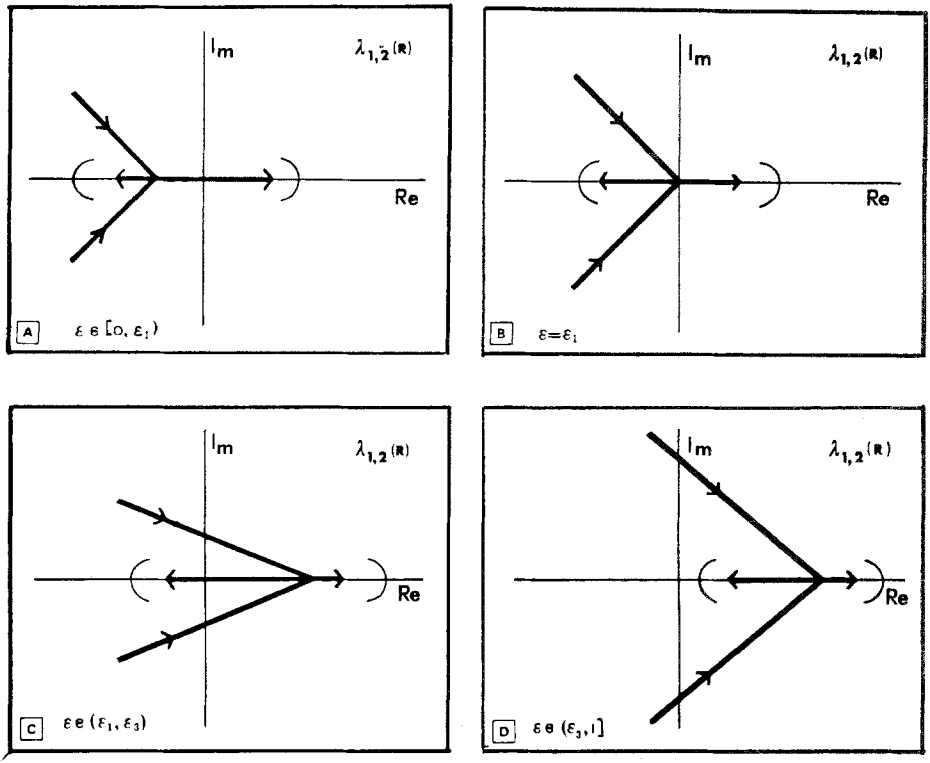

Fig. 2. The behavior of $\lambda_{1,2}(R, \epsilon)$, at fixed ϵ, pictured as linear. The brackets on the real axis indicate that the range $\{\lambda_{1,2}(R)/R \geqslant R_s(\epsilon)\}$ is finite, and that for $\epsilon > \epsilon_3$ (Fig. 2D) it does not contain zero.

crossing the imaginary axis at different points on their way, depending on the interval in which ϵ is chosen.

At the critical points ϵ_1 and ϵ_3 the situation is

(iv) $\epsilon = \epsilon_1$

$\lambda_{1,2}(R)$ become real and coincident in zero, for $R = R_s(\epsilon) = R_h(\epsilon)$ (Fig. 2B). We verified numerically that the P_σ's undergo a stationary bifurcation also in this limit case, because they originate the stable $P_{\sigma\tau}$'s.

(v) $\epsilon = \epsilon_3$

There is no value of R at which $P_{\sigma\tau}(R, \epsilon)$ exist; moreover there is numerical evidence that the range $\{\lambda_{1,2}(R, \epsilon_3)/R > R_h(\epsilon_3)\}$ has its lower bound in zero, in the sense that $\lambda_2(R) \to 0$ as $R \to \infty$. For this reason no stationary bifurcation for P_σ takes place.

In conclusion, by explicit computation of the matrix $L_\sigma(R, \epsilon)$ at the point P_σ, we can argue that the whole interesting phenomenology con-

nected with the four fixed points $P_{\sigma\tau}$, studied in Refs. 4 and 5 for $\epsilon = 0$, is a priori possible only for $\epsilon \in [0, \epsilon_3)$, i.e., for values of ϵ for which $R_s(\epsilon)$ is finite, and $P_{\sigma\tau}(R, \epsilon)$ exist. On the other hand, the phenomenology observed for $\epsilon = 1$ in Ref. 6, with points bifurcating into orbits, with orbits bifurcating into tori, is a priori possible only for $\epsilon \in (\epsilon_1, 1]$, i.e., for values of ϵ for which $P_\sigma(R, \epsilon)$ undergoes a Hopf bifurcation as R increases. For $\epsilon \in (\epsilon_1, \epsilon_3)$, while we have observed numerically a phenomenology of bifurcations of periodic orbits generated both by P_σ and by $P_{\sigma\tau}$, no chaotic behavior has been observed. We will discuss this intermediate situation in Section 7.

The different bifurcations that take place as R varies, fixing ϵ, are pictured in Fig. 3.

We studied numerically the stability of the stationary solutions $P_{\sigma\tau}$, without computing explicitly the critical values of R for $P_{\sigma\tau}$.

(i′) fixing $0 \leqslant \epsilon \leqslant \epsilon_1$

$P_{\sigma\tau}$ arise stable and attractive at $R = R_s(\epsilon)$ (Fig. 3A). As R increases, they undergo a direct Hopf bifurcation because a pair of complex conjugate eigenvalues $\gamma_{1,2}$ of the Liapunov matrix at $P_{\sigma\tau}, L_{\sigma\tau}(R, \epsilon)$ crosses the imaginary axis at $R = \rho_0(\epsilon)$. The $P_{\sigma\tau}$'s bifurcate then into four symmetrical periodic orbits, $H^0_{\sigma\tau}$, one around each $P_{\sigma\tau}$; the orbits have period $\Pi(H^0_{\sigma\tau}) \cong 2\pi/\mathrm{Im}(\gamma_{1,2})$, as predicted by the bifurcation theory[17].

(ii′) fixing $\epsilon_1 < \epsilon < \epsilon_3$

$P_{\sigma\tau}$ arise unstable at $R = R_s(\epsilon)$, with a pair of conjugate eigenvalues $\gamma_{3,4}$ of the Liapunov matrix $L_{\sigma\tau}$ placed in the right half-plane, and the other five γ_i, $i = 1, 2, 5, 6, 7$ in the left one. As R increases, the pair $\gamma_{3,4}$ crosses the imaginary axis from right to left at $R = R_2(\epsilon)$, while another pair, $\gamma_{1,2}$ crosses the imaginary axis from left to right at $R = \rho_0(\epsilon)$. We saw numerically that $R_2(\epsilon) < \rho_0(\epsilon)$ for $\epsilon \in (\epsilon_1, \epsilon_2)$, and that $\rho_0(\epsilon) < R_2(\epsilon)$ for $\epsilon \in (\epsilon_2, \epsilon_3)$, where $\epsilon_2 \cong 0.31540$ is such that $R_2(\epsilon_2) = \rho_0(\epsilon_2)$. We have then a subpartition of (ϵ_1, ϵ_3) in two intervals:

Fixing $\epsilon_1 < \epsilon < \epsilon_2$ (Fig. 3B)

$P_{\sigma\tau}$ arise unstable at $R = R_s(\epsilon)$, and become stable at $R = R_2(\epsilon)$; the now stable $P_{\sigma\tau}$'s lose stability then, at $R = \rho_0(\epsilon)$, bifurcating into the stable periodic orbits $H^0_{\sigma\tau}$.

Fixing $\epsilon_2 < \epsilon < \epsilon_3$ (Fig. 3C)

$P_{\sigma\tau}$ arise unstable at $R = R_s(\epsilon)$, and then undergo a direct Hopf bifurcation generating four unstable orbits $H^0_{\sigma\tau}$. In this way the $P_{\sigma\tau}$'s become "twice" unstable, i.e., with two pairs of complex conjugate eigenvalues for $L_{\sigma\tau}$ in the right half-plane. As R increases beyond $R_2(\epsilon)$ and the pair $\gamma_{3,4}$ crosses the imaginary axis from right to left, $P_{\sigma\tau}$ may undergo another bifurcation, but we were not able to understand what kind.

Any attempt to look for a stable periodic orbit bifurcated via Hopf at $R = R_2(\epsilon)$, as R decreases, for $\epsilon < \epsilon_2$, has been unsuccessful, so that we

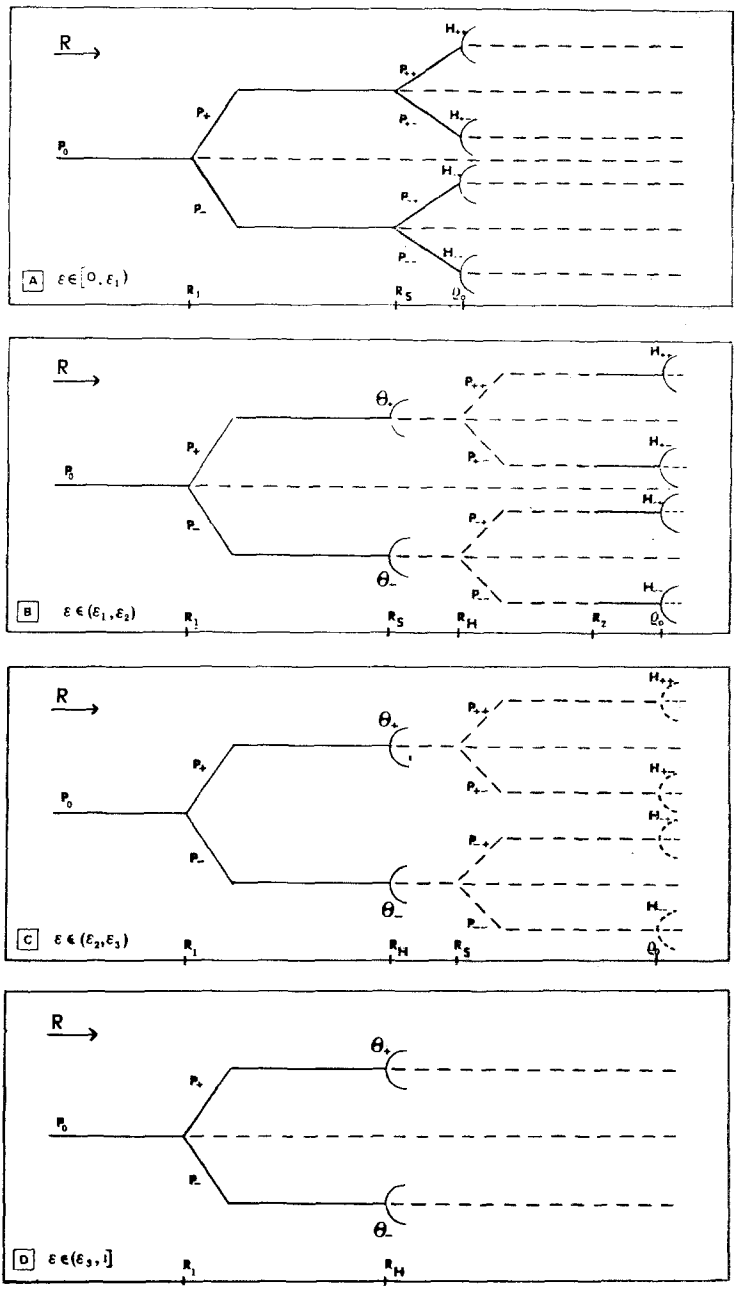

Fig. 3. Graphical summary (not in scale) of the bifurcations undergone by P_σ and $P_{\sigma\tau}$ as R varies. A continuous line —— indicates attractors, a broken line - - - indicates repulsors; the sign ——< indicates a stationary bifurcation, and ——⊂ a direct Hopf bifurcation.

would exclude that this is a direct bifurcation (see Section 7 for the case $\epsilon = 0.3$).

4. SEQUENCES OF PERIOD-DOUBLING BIFURCATIONS

As mentioned in Section 2, unlike the seven-mode model, in the five-mode one, i.e., at $\epsilon = 0$, the onset of turbulence is due to the exhaustion of two infinite sequences of bifurcations, related to two infinite sequences of periodic orbits, $\{H^i\}$ and $\{A^i\}$.

We will call $\rho_i(\epsilon)$ the value of R, fixed ϵ, at which the periodic orbit H^{i-1} bifurcates into the periodic orbit H^i, doubled in period and winding up twice around H^{i-1}; $\mu_i(\epsilon)$ will denote the value of R, fixed ϵ, at which the orbit A^{i-1} loses stability bifurcating into the periodic orbit A^i, also doubled in period and winding up twice around A^{i-1}. Since the sequences $\{\rho_i(0)\}$ and $\{\mu_i(0)\}$ are compatible with Feigenbaum's conjecture [8], in Ref. 5 two values are estimated, ρ_∞ and μ_∞, at which, respectively, the sequences $\{H^i\}$ and $\{A^i\}$ exhaust themselves.

Still in Ref. 5 a chaotic behavior is observed for $\mu_\infty < R < R_\Gamma'$, that is up to a value of R at which a periodic orbit Γ arises, which seems to exist stable and attractive for any larger value of R. We found that this R range of turbulence is actually broken by another sequence of period-doubling bifurcations, giving rise to a sequence of orbits $\{C^i\}$, which in turn is very likely to be infinite.[3]

It is rather puzzling that these phenomena do not appear at all in the seven-mode model, i.e., at $\epsilon = 1$. The thing can be explained first observing that all of the critical values $\rho_i(\epsilon)$, regarding the sequence $\{H^i\}$, go to infinity with $\epsilon \uparrow \epsilon_3$. In fact the first orbit of the sequence, H^0, arises via a Hopf bifurcation from the stationary solutions $P_{\sigma\tau}$, which in turn arise at $R_s(\epsilon)$, and we saw in Section 3 that $R_s(\epsilon) \to +\infty$ as $\epsilon \uparrow \epsilon_3$. Moreover, looking at Fig. 4, one can see that turbulence is actually "swallowed" by the postturbulence periodic orbit Γ, whose "birth value" $R_\Gamma^a(\epsilon)$ is finite for every value of ϵ. [We will see the fate of $\Gamma(\epsilon)$ in the next section.]

Now, considering the matter in detail, let us sketch the major features concerning the sequences $\{H^i(\epsilon)\}$, $\{A^i(\epsilon)\}$, $\{C^i(\epsilon)\}$ as ϵ is increased from zero.

Consider first the sequence $\{H^i\}$. It gets rapidly squashed against H^0. In fact, it is not difficult to verify that, while for $\epsilon = 0.15$ the orbit H^2 is easy to find, for $\epsilon = 0.20$ it is not detectable any more even if the orbit H^1 continues to bifurcate through -1. Furthermore, one can easily check that $\rho_2(\epsilon)$ tends to $\rho_1(\epsilon)$ as ϵ tends to ϵ_1.

[3] Each of the sequences $\{H^i\}$, $\{A^i\}$, $\{C^i\}$, has to be regarded as four symmetrical sequences $\{H^i_{\sigma\tau}\}$, $\{A^i_{\sigma\tau}\}$, $\{C^i_{\sigma\tau}\}$, undergoing identical behavior, as mentioned in Section 2.

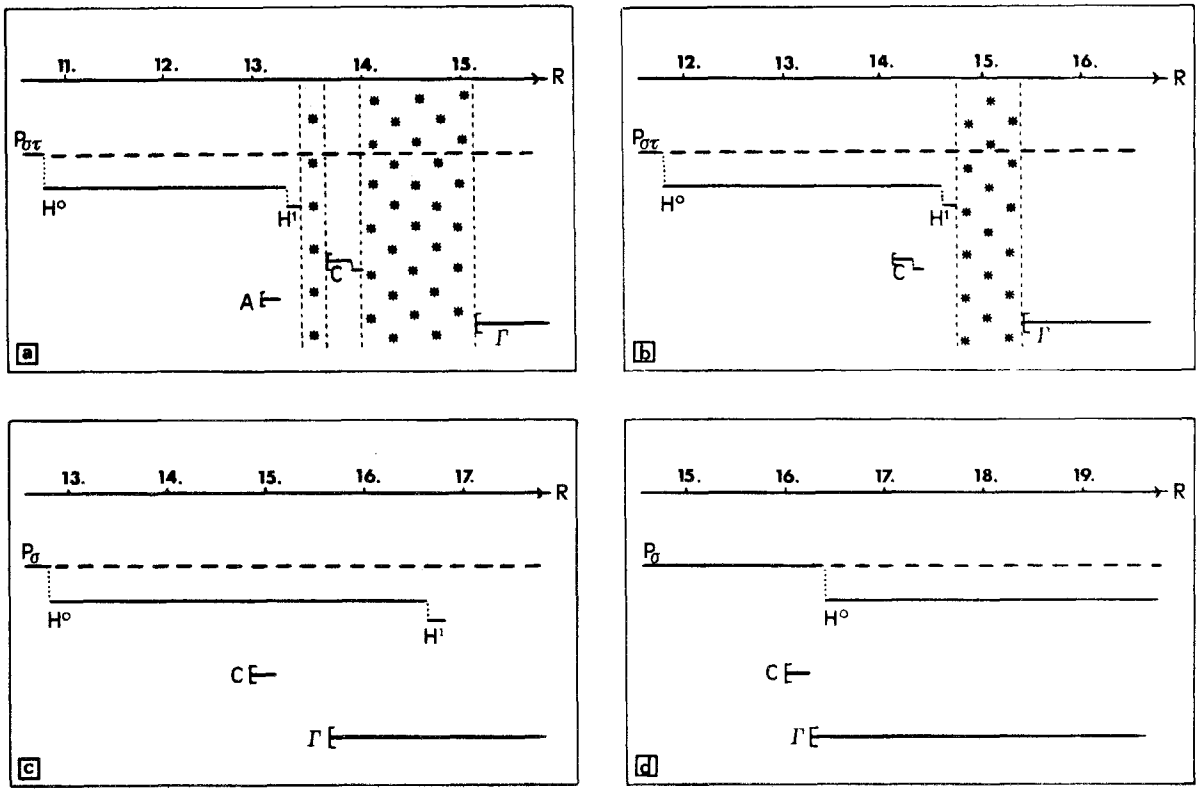

Fig. 4. Graphical summary of the phenomenology exhibited by system (3.1), fixing ϵ, as R varies: (A) at $\epsilon = 0.1$ the system shows two ranges of turbulence (just like at $\epsilon = 0$; see Fig. 1A); (B) at $\epsilon = 0.15$ the system shows one range of turbulence; (C) and (D) at $\epsilon = 0.2$ and $\epsilon = 0.25$ no chaotic behavior is shown by the system. Here everything is in scale.

Another feature about H^0 can be observed fixing ϵ in the range (ϵ_2, ϵ_3), where $\epsilon_2 = 0.3154$. The $H^0_{\sigma\tau}$'s arise unstable from unstable $P_{\sigma\tau}$ at $R = \rho_0(\epsilon)$ (see Fig. 3c). This fact seems quite interesting because it is an example of a direct Hopf bifurcation from unstable fixed points into unstable periodic orbits. As R increases, the $H^0_{\sigma\tau}$'s gain stability at $R = R_3(\epsilon)$ and then they become again unstable at $R = \varrho_1(\epsilon)$ because of an eigenvalue -1. For R slightly greater than $\varrho_1(\epsilon)$, any randomly chosen initial data in a neighborhood of H^0 is rapidly attracted by Γ. We cannot exclude, though, that at $\varrho_1(\epsilon)$ we have an inverse bifurcation to an unstable orbit of double period.

As far as the sequence $\{A^i\}$ is concerned, there is numerical evidence that their R range of existence tends to vanish as ϵ increases from zero. We have verified that for $\epsilon = 0.15$ the stability R-range of A^0 is about 0.0013, while the same range for $\epsilon = 0$ is about 0.015.

Also the R range of stability of the sequence $\{C^i\}$ vanishes as ϵ increases, but in a different way.

For $0 \leqslant \epsilon \leqslant 0.32$ the periodic orbit C^0 arises stable, together with an unstable C^*, at $R = \nu_0(\epsilon)$. It then becomes unstable at $R = \nu_1(\epsilon)$, because a real eigenvalue of the Liapunov matrix of its Poincaré map leaves the unit circle through -1. The next orbit of the sequence, C^1, however, becomes indetectable for values of ϵ greater than 0.15, as its range of stability gets smaller and smaller.

The behavior of C^0 suddenly changes for $\epsilon > 0.32$. In fact its stability range quickly vanishes because a pair of complex conjugate eigenvalues crosses the unit circle.

For $\epsilon = 0.34$ C^0 arises unstable, and remains unstable for every value of R at which it is detectable.

To notice the fact that for $\epsilon \geqslant 0.32$, we have $\nu_0(\epsilon) < R_s(\epsilon)$, which means that the orbit C^0 exists for values of (R, ϵ) at which the stationary solutions $P_{\sigma\tau}$ do not exist. Moreover, the unstable C^0 has been followed in ϵ up to $\epsilon = 0.347$, i.e., a value of ϵ at which the $P_{\sigma\tau}$'s do not exist for any R [in fact $R_s(\epsilon) \to +\infty$ as $\epsilon \uparrow \epsilon_3 \cong 0.3464 \ldots$]. Hence the four orbits $C^0_{\sigma\tau}$ are not strictly connected with the four stationary solutions $P_{\sigma\tau}$, as it may appear at $\epsilon = 0$.

5. A PERIODIC ORBIT COMMON TO THE TWO MODELS

Two stable periodic orbits Γ_+ and Γ_-, each one invariant under the symmetry (β), and transformed into the other by (α) or (γ), are present for any value of $\epsilon \in [0, 1]$. We will refer to both of them simply as Γ in the following, as they undergo identical behavior, owing to the symmetries of the system.

Table I

ϵ	$R'_\Gamma(\epsilon)$	$R''_\Gamma(\epsilon)$
0	14.9	$+\infty$
0.1	15.1	$+\infty$
0.3	16.7	$+\infty$
0.5	20.6	$+\infty$
0.7	33.5	105.5
0.9	44.4	593.9
1	63.3	197.5

In different ranges of ϵ, however, Γ plays quite different roles. At $\epsilon = 1$ (see Ref. 6), it is a "preturbulence" orbit, which becomes unstable at $R = 197.5$ bifurcating into a stable 2-torus $T(\Gamma)$, which in turn becomes unstable. At $\epsilon = 0$, on the other hand (see Refs. 4 and 5) Γ is a "postturbulence" orbit which is stable and attracting $\forall R > 14.95$.[4]

Introducing the notation $R'_\Gamma(\epsilon)$, $R''_\Gamma(\epsilon)$, respectively, for the least and the largest values of R, fixed ϵ, at which Γ exists and is attracting, we numerically determined the scheme shown in Table I, displaying different strange features. While $R'_\Gamma(\epsilon)$ looks like a nicely increasing function, $R''_\Gamma(\epsilon)$, far from showing any regularity, seems to overtake infinite value for some ϵ. The explanation lies in the behavior of the eigenvalues of the Liapunov matrix of the Poincaré map for Γ, which will be called $M(R, \epsilon)$.

Let us first consider the function $R'_\Gamma(\epsilon)$.

For values of $\epsilon \leqslant 0.3$, $R'_\Gamma(\epsilon)$ represents the least value of R for which Γ exists; in fact one can see numerically that a real eigenvalue of M tends to join the unit circle at $+1$, as R decreases to $R'_\Gamma(\epsilon)$; we have verified numerically that with decreasing R toward $R'_\Gamma(\epsilon)$ the stable periodic orbit Γ coalesces with an unstable orbit Γ^* (as predicted by the general bifurcation theory[9]), and that for $R < R'_\Gamma(\epsilon)$ the orbit is no longer present, so that $R'_\Gamma(\epsilon)$ is a "birth" value for Γ, let us call it $R^a_\Gamma(\epsilon)$.

At other values for ϵ, though, $R'_\Gamma(\epsilon)$ is no longer a "birth" value for the orbit Γ:

At $\epsilon = 0.5$, for instance, $R'_\Gamma(\epsilon)$ represents the least value of R for which Γ is stable; with decreasing R *beyond* $R'_\Gamma(\epsilon)$, an eigenvalue of M actually crosses the unit circle at $+1$, so that for $R < R'_\Gamma(\epsilon)$, Γ exists, but it is unstable. We did not investigate what kind of bifurcation takes place at $R'_\Gamma(\epsilon)$ for this value of Γ; however, as R decreases from $R'_\Gamma(\epsilon)$, we see numerically that another eigenvalue of M tends to join the unit circle at

[4] The presence of a stable periodic orbit for high values of the parameter in a dissipative system of this kind is not surprising: for the Lorenz model, for instance, it has been rigorously shown by K. Robbins.[10]

$+1$, and the now unstable Γ coalesces at $R = R_\Gamma^\alpha(0.5) \cong 20.19$ with a "twice" unstable Γ^* (i.e., with two real eigenvalues out of the unit circle); this latter is the value of R to be regarded as the birth point of Γ at $\epsilon = 0.5$.

At $\epsilon = 0.7$ Γ still loses stability as R decreases beyond $R_\Gamma'(\epsilon)$ with a real eigenvalue actually crossing the unit circle at $+1$.

At $\epsilon = 0.9$ and $\epsilon = 1$. Γ becomes unstable with decreasing R, as a pair of complex conjugate eigenvalues of M crosses the unit circle for $R = R_\Gamma'(\epsilon)$.

We think that a birth value $R_\Gamma^\alpha(\epsilon)$ for Γ still exists at these values of ϵ, but as Γ rapidly becomes very unstable with decreasing R, it is difficult to follow it continuously and to determine $R_\Gamma^\alpha(\epsilon)$.

To the unexpected nonmonotone trend of $R_\Gamma''(\epsilon)$, it is reasonable to say that $R_\Gamma''(\epsilon)$ is actually piecewise monotone, and the intervals of monotonicity can be determined again looking at the behavior of the eigenvalues $\xi_1, \ldots, \xi_6$ of $M(R, \epsilon)$. More precisely, our numerical investigations suggest considering four ϵ intervals:

(a) $0 \leqslant \epsilon < \epsilon_4$

$R_\Gamma''(\epsilon)$ is presumably infinite. For any R greater than $R_\Gamma'(\epsilon)$ all the eigenvalues of M are inside the unit circle, and Γ is stable and attractive.

For $\epsilon = \epsilon_4$, which seems numerically to be about 0.5, a real eigenvalue, ξ_3 tends to $+1$ as R tends to infinity.

(b) $\epsilon_4 < \epsilon < \epsilon_5$

Here $R_\Gamma''(\epsilon)$ is a decreasing function. Now the eigenvalue ξ_3 actually crosses the unit circle for some finite value of R, and Γ becomes unstable.

For $\epsilon = \epsilon_5$, $R_\Gamma''(\epsilon)$ has a minimum as a second eigenvalue of M, say ξ_1, goes out of the unit circle through $+1$ at the same time of ξ_3. We did not determine ϵ_5.

(c) $\epsilon_5 < \epsilon < \epsilon_6$

$R_\Gamma''(\epsilon)$ is an increasing function. Γ becomes unstable at $R = R_\Gamma''(\epsilon)$ because ξ_1 crosses the unit circle at $+1$. Such a bifurcation, however, has not been investigated. We have instead found that $0.83 < \epsilon_6 < 0.85$. In fact, for $\epsilon = 0.83$ Γ loses stability at $R = R_\Gamma''(.83) \cong 1750.0$ because of the real eigenvalue ξ_1 becoming greater than $+1$, while for $\epsilon = 0.85$. Γ becomes unstable at $R = R_\Gamma''(0.85) \cong 2634.0$ because of the pair of complex conjugate eigenvalues (ξ_1, ξ_2) crossing the unit circle. For $0.835 \leqslant \epsilon \leqslant 0.845$, on the other hand, Γ is still stable at $R = 3300.$, with period $\Pi(\Gamma) \cong 0.060$, and since the period of Γ is a decreasing function of R and Γ is a very large orbit, it is not worth integrating it numerically for larger values of R.

(d) $\epsilon_6 < \epsilon \leqslant 1$

$R_\Gamma''(\epsilon)$ is a decreasing function, and fixing ϵ in this range, Γ loses stability at $R = R_\Gamma''(\epsilon)$ with a pair of complex conjugate eigenvalues, ξ_1 and ξ_2 crossing the unit circle; as expected from the general bifurcation theory,[2] Γ bifurcates into a stable 2-torus $T(\Gamma)$, as R increases beyond $R_\Gamma''(\epsilon)$.

Remark. For R slightly greater than $R'_\Gamma(\epsilon)$ all the eigenvalues of M are inside the unit circle. We have then a picture for these eigenvalues, which is quite similar to the one in Section 3 (Fig. 2), concerning eigenvalues of the Liapunov matrix for the stationary solutions P_σ. Observing that the role played there by the imaginary axis is here played by the unit circle, we still have two complex conjugate eigenvalues ξ_1, ξ_2 that become real as R increases. Depending on the value of ϵ that has been fixed, the pair will become real outside the unit circle (d) or inside the unit circle (a, b, c). In this latter case one of the two now real eigenvalues, ξ_1, increases in a finite range: if this range contains $+1$ we have (c). Otherwise, we have (b) when the range of another eigenvalue, $\xi_3(R)$, contains $+1$, and (a) when it does not contain $+1$ either.

6. PERIODIC SOLUTIONS FROM THE SEVEN-MODE MODEL

In Ref. 6 the model is studied at $\epsilon = 1$; in this case a stochastic behavior is observed at large values of R, when no simple attractor is present. Two symmetric stable periodic orbits Θ_σ, bifurcated from the stationary solutions P_σ via a Hopf bifurcation at $R = R_h(1)$, and two other symmetric orbits Γ_τ, lose stability bifurcating into two 2-tori $T(\Theta_\sigma)$, $T(\Gamma_\tau)$, respectively, as R increases beyond certain critical values. We have already seen in Section 5 that Γ is the postturbulence orbit of the five-mode model. Studying the two functions $R'_\Gamma(\epsilon)$ and $R''_\Gamma(\epsilon)$ and their different meanings to the bifurcations of Γ, we also saw how its role changes as ϵ increases from zero to one.

For what concerns the orbits Θ_σ, present in the interval $(\epsilon_1, 1]$, we have not performed an analogous study as ϵ varies, limiting ourselves to investigating their behavior at $\epsilon = 0.3$. Referring to the next section for the results of such study, let us remark here something about their period, $\Pi(\Theta_\sigma)$. Using Hopf's theorem to predict the period of the orbits Θ_σ, we have that $\Pi(\Theta) = 2\pi/\lambda_0$, λ_0 being the imaginary part of the eigenvalues of $L_\sigma(R, \epsilon)$ crossing the imaginary axis as a pair of complex conjugate numbers. Since $\lambda_0 \to 0$ as $\epsilon \downarrow \epsilon_1$ (see Section 3 and Fig. 2), the period of Θ tends to infinity as ϵ decreases to ϵ_1.

Still in Ref. 6, four other stable periodic orbits are studied, $\chi_{1,2}$ and $\psi_{1,2}$, that do not seem to bifurcate into any other attractor as they lose stability with increasing R (see Section 2); we have verified that these orbits tend to become unstable for every R as ϵ decreases from $\epsilon = 1$. More precisely χ_1 and χ_2 are two symmetric periodic orbits, each one invariant under symmetry (γ) and transformed in the other by (α) or (β); as they undergo identical behavior, owing to the symmetry of the system, they will be referred to as χ in the following. ψ_1 and ψ_2 are invariant under (α) and each

one is transformed into the other by (β) or (γ), so that they will be referred to as ψ in the following. Keeping, as in Section 5, the notation $R'_\chi(\epsilon)$ and $R'_\psi(\epsilon)$, respectively, for the least value of R, fixed ϵ, for which χ and ψ are stable, and $R''_\chi(\epsilon)$, $R''_\psi(\epsilon)$ for the largest values of R for which, respectively, χ and ψ exist and are attractors, we have from Ref. 6, that $R'_\chi(1) \cong 141.7$ and $R''_\chi(1) \cong 248.2$, while $R'_\psi(1) \cong 146.61$ and $R''_\psi(1) \cong 166.59$. It has been verified numerically that the range of stability $[R''(\epsilon) - R'(\epsilon)]$ rapidly decreases with ϵ in both cases. As far as χ is concerned, there is numerical evidence that

$$\left[R''_\chi(\epsilon) - R'_\chi(\epsilon)\right] \underset{\epsilon \downarrow \epsilon_7}{\longrightarrow} 0$$

where $\epsilon_7 \cong 0.85$. A similar trend is observed for ψ, but we did not determine a value for ϵ at which the R range of stability for ψ vanishes, because the strong dependence of ψ on ϵ made it both difficult and expensive to follow ψ continuously as ϵ decreases from $\epsilon = 1$.

7. AN INTERMEDIATE MODEL: $\epsilon = 0.3$

As mentioned in Section 3, if we consider the system (3.1) regarded at fixed $\epsilon \in (\epsilon_1, \epsilon_3)$ as a one-parameter family of differential equations (the parameter being R), we have a superposition of the phenomenologies of the five-mode model and of the seven-mode one. Moreover, for these values of ϵ, no chaotic behavior is observed at any value of R. We think then it is worth describing rather in detail the asymptotic behavior of solutions of the system at $\epsilon = 0.3$, summarized graphically in Fig. 5. The dependence on ϵ of the critical values $R_i(\epsilon)$ will not thus be stressed any more in the present section.

As expected by rigorous computations and verified numerically (see Section 3, and Fig. 3B), we have the following:

(i) $0 \leqslant R \leqslant R_1 \cong 2.74$

One stationary solution, P_0 is present, stable, and by numerical evidence globally attractive.

(ii) $R_1 < R < R_h \cong 8.79$

Two more stationary solutions P_σ are present, bifurcated at $R = R_1$ from P_0, therefore now unstable; the P_σ's are symmetric, stable and attractive. ($\sigma = \pm$; for coordinates see Section 3.)

(iii) $R_h \leqslant R \leqslant R_s \cong 12.32$

As R increases beyond R_h, a pair of complex conjugate eigenvalues of the Liapunov matrix for P_σ crosses the imaginary axis, and two stable periodic solutions Θ_σ arise via a direct Hopf bifurcation, each around one of the now unstable P_σ's.

(iv) At $R = R_s$

One of two positive eigenvalues of the Liapunov matrix for P_σ crosses the imaginary axis from right to left, and P_σ bifurcate into four unstable stationary solutions $P_{\sigma\tau}$, two from each P_σ.

The other phenomena taking place as R varies have been studied numerically.

The orbits Θ_σ, which will be now on referred to as Θ, exhibit an interesting feature: either they exist and are attractors, or they do not exist at all. In fact Θ appears stable via a Hopf bifurcation at $R = R_h$, with period $\Pi(\Theta) \cong 12.05 \cong 2\pi/|\mathrm{Im}\,\lambda_1|$, as predicted by the general bifurcation theory. Numerical studies show that the eigenvalues of its Poincaré map keep inside the unit circle for values of R up to $R = 19.660$, when a real eigenvalue joins the unit circle at $+1$. We verified that at this value of the parameter, Θ coalesces with an unstable periodic orbit Θ^*, which is present at the same time. The two critical values of R can thus be regarded, respectively, as points of "birth" and "death," R_Θ^α and R_Θ^ω, for Θ, which therefore exists and is an attractor for $8.79 \cong R_\Theta^\alpha \leqslant R \leqslant R_\Theta^\omega \cong 19.66$.

So far, the phenomenology connected with the two points P_σ. Consider now the four stationary solutions $P_{\sigma\tau}$, bifurcated unstable from unstable P_σ at $R = R_S$ (Fig. 3B). They become stable at $R = R_2 \cong 16.85$, when a pair of complex conjugate eigenvalues of $L_{\sigma\tau}$ crosses the imaginary axis from right to left. We can exclude that a direct Hopf bifurcation takes place, since any numerical attempt to find a stable periodic orbit of the expected period around $P_{\sigma\tau}$ for R slightly smaller than R_2 gave no result. We can guess that an inverse Hopf bifurcation takes place at $R = R_2$, and an unstable periodic orbit is present around each $P_{\sigma\tau}$ for $R > R_2$, but we could not verify it.

$R_2 < R < \rho_0 \cong 27.37$

$P_{\sigma\tau}$ are stable up to $R = \rho_0$, when a direct Hopf bifurcation takes place and four stable symmetric periodic orbits $H_{\sigma\tau}^0$ appear, each around one $P_{\sigma\tau}$.

At $R = \rho_1 \cong 33.19$ $H_{\sigma\tau}^0$ becomes unstable as a real eigenvalue of its Poincaré map crosses the unit circle at -1; unlike the case $\epsilon = 0$ (see Refs. 4 and 5), H^0 does not seem to bifurcate into a stable orbit of doubled period. For R slightly greater than ρ_1, initial data near the now unstable H^0 are attracted by other attractors present at the same time.

$17.57 \cong R_C^\alpha < R < R_C'' \cong 17.68$; In this range of R another periodic orbit is present, C, which appears at $R = R_C$ together with an unstable one, C^* (i.e., as $R \downarrow R_C^\alpha$, C coalesces with C^*). At $R = R_C''$ a real eigenvalue of the Poincaré map for C crosses the unit circle at -1, but no period-doubling bifurcation seems to take place. (C must actually be regarded as four orbits symmetrically placed.)

The periodic orbit Γ arises at $R = R_\Gamma^\alpha \cong 16.73$ together with unstable Γ^*, and remains stable and attracting for every value of R that we have

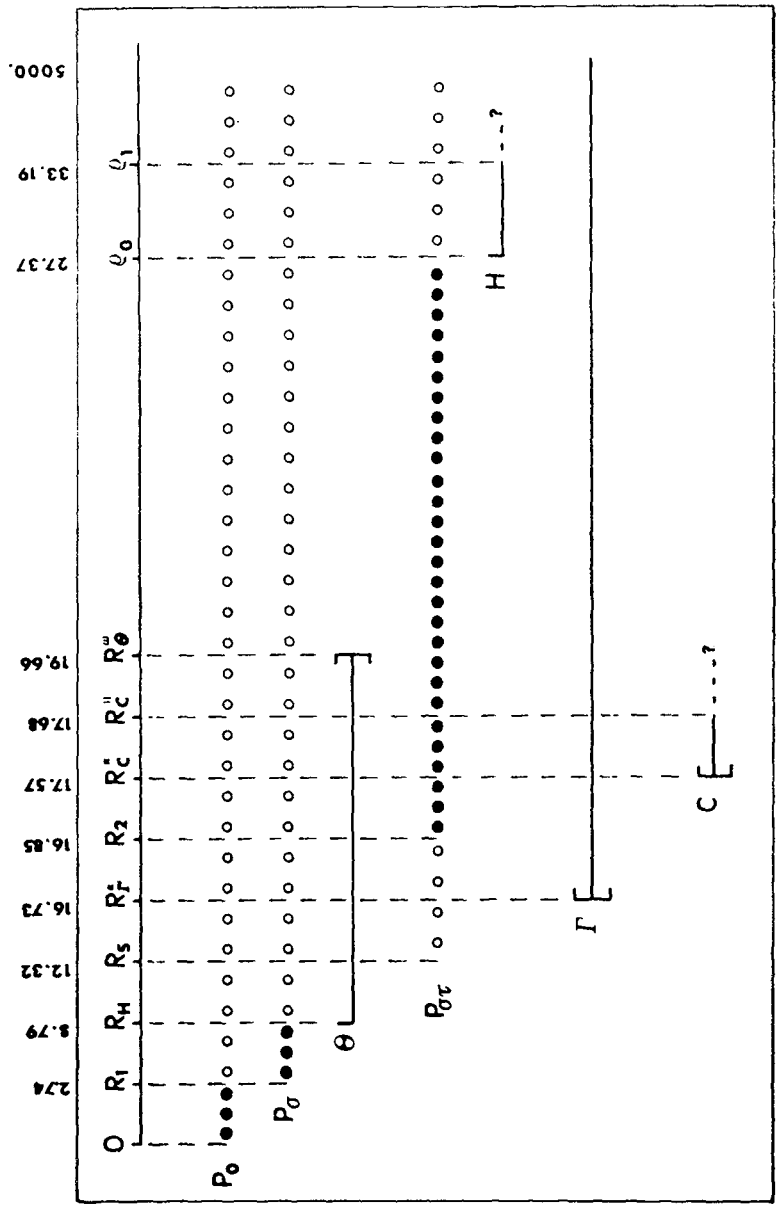

Fig. 5. Graphical summary (not in scale) of the phenomenology exhibited by system (3.1) for $\epsilon = 0.3$ as R varies. Notation as in Fig. 1.

investigated (up to $R = 5000$). As R increases the period $\Pi(\Gamma)$ decreases, and for large values of the parameter any random initial point is rapidly attracted by Γ.

As mentioned in Section 4, the orbit A, which for $\epsilon = 0$ gives rise to an infinite series of period-doubling bifurcations, is no longer detectable at this value of ϵ.

At $\epsilon = 0.3$, therefore, no chaotic behavior is observed. At every value of R the nonwandering set $\Omega(R)$ consists of a finite number of stationary solutions and periodic orbits, at least one of which is stable and attracting, as it is possible to verify integrating system (3.1) with random initial data.

8. CONCLUSIONS

In this paper we have studied the transition from a 5-mode model of truncated Navier–Stokes equations, to a 7-mode one. The two models, the latter extending the former, exhibit two rather different phenomenologies, and this motivated our study. In fact, setting a weight ϵ on the two added modes, x_6 and x_7, one can see what their relevance is to the whole phenomenology.

The main results of the study are synthesized in Fig. 6, where it is possible to check how crucial the critical value ϵ_3 is, since the phenomenology connected with the four stationary solutions $P_{\sigma\tau}$ goes to infinity as ϵ tends to ϵ_3 (curves R_s, R_2, ρ_0).

The other two infinite sequences of periodic orbits, $\{A^i\}$ and $\{C^i\}$, present in the 5-mode model and connected with the onset of turbulence, disappear because their R-range of stability vanishes as ϵ increases from zero. For this reason their critical curves are not pictured in Fig. 6, but it is worth saying that for $\epsilon = 0.34$ they are both already gone.

Turbulence disappears in the same way as ϵ increases from zero. It develops in a range of R which is finite in the 5-mode model ($\epsilon = 0$), shifts to higher R's as ϵ increases, and vanishes canceled by the periodic orbit Γ, whose birth function, $R_\Gamma^\alpha(\epsilon)$ overtakes finite values for every $\epsilon \in [0, 1]$. As ϵ tends to 1, turbulence develops at high values of R, when no other simple attractor is present.

The critical curves for the orbits χ and ψ of the 7-mode model are not present in Fig. 6, because their behavior is analogous to $\{A^i\}$ and $\{C^i\}$, that is, their R ranges of stability vanish as ϵ decreases from one. For $\epsilon = 0.8$ they are both already gone.

We did not investigate in more detail (except for the strange $\epsilon = 0.3$ case) the behavior of system (3.1) at intermediate values of ϵ, even though it might show interesting phenomena not present at $\epsilon = 0$ nor at $\epsilon = 1$. We preferred to understand thoroughly how the 5-mode phenomenology disappears and how the onset of the 7-mode one takes place.

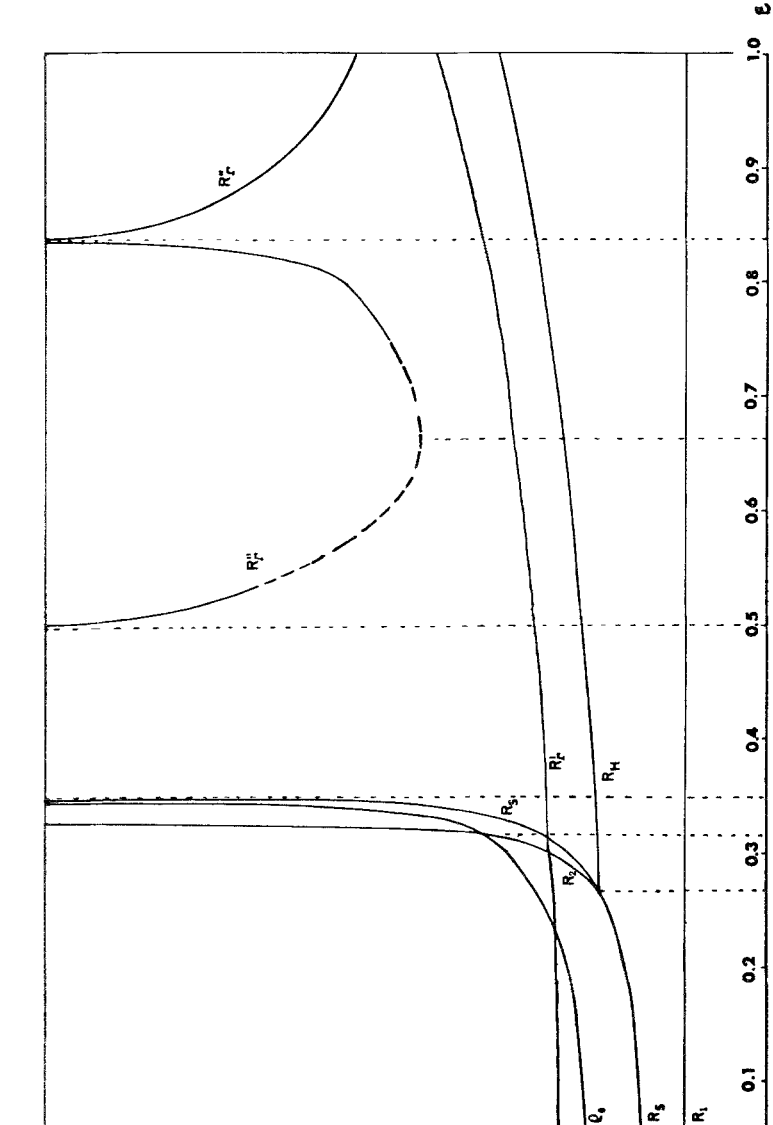

Fig. 6. Critical curves $R(\epsilon)$ separating regions of the plane (R, ϵ) (in semilogarithmic scale), characterized by different asymptotic behavior of system (3.1). Three of the curves, namely, R_1, R_3, and R_H, are rigorous. The others are fitted on numerical data, so that they are not necessarily C^1 as pictured. In particular the branch of $R_1''(\epsilon)$ around its minimum ϵ_5 is fitted on very few data. The curve's meanings, in terms of bifurcations, at fixed ϵ and increasing R, are as follows: R_1: stationary solution P_0 bifurcates into two stationary solutions P_σ; R_3: stationary solutions P_σ bifurcate into four stationary solutions $P_{\sigma\tau}$; R_H: stationary solutions P_σ Hopf-bifurcate into periodic orbits Θ_σ; ρ_0: stationary solutions $P_{\sigma\tau}$ Hopf-bifurcate into periodic orbits $H_{\sigma\tau}^0$; R_2: unstable $P_{\sigma\tau}$ become stable; R_Γ': periodic orbit Γ either arises stable or becomes stable; R_Γ'': periodic orbit Γ becomes

ACKNOWLEDGMENTS

This note developed under continuous discussions with V. Franceschini. The problem was suggested by G. Gallavotti. It is my pleasure to thank them both for their participation and constant encouragements. I wish also to thank the staff of the Centro di Calcolo dell'Università di Modena for friendly technical assistance.

REFERENCES

1. R. H. G. Hellemann, Self-generated Chaotic Behavior in Nonlinear Mechanics, in *Fundamental Problems in Statistical Mechanics*, Vol. 5, pp. 165–233, E. D. G. Cohen, ed. (North Holland, Amsterdam, 1980).
2. D. Ruelle and F. Takens, On the Nature of Turbulence, *Commun. Math. Phys.* **20**:167 (1971).
3. C. Boldrighini, *Lezioni di fluidodinamica* Quaderno dei Gruppi di Ricerca Matematica del C.N.R. Roma (1979).
4. C. Boldrighini and V. Franceschini, A Five-Dimensional Truncation of the Plane Incompressible Navier–Stokes Equations, *Commun. Math. Phys.* **64**:150 (1979).
5. V. Franceschini and C. Tebaldi, Sequences of Infinite Bifurcations in a 5-Mode Truncation of the Navier–Stokes Equations, *J. Stat. Phys.* **21**:707 (1979).
6. V. Franceschini and C. Tebaldi, A Seven-Mode Truncation of the Plane Incompressible Navier–Stokes Equations. *J. Stat. Phys.* **25**:397 (1981).
7. J. Marsden and M. McCracken, *The Hopf Bifurcation and its Applications* Appl. Math. Sciences, Vol. 19 (1976).
8. M. J. Feigenbaum, Quantitative Universality for a class of Nonlinear Transformations, *J. Stat. Phys.* **19**:25 (1978).
9. P. Brunowsky, One-Parameter Families of Diffeomorphisms, *Lecture Notes in Math.* **206**:(1971).
10. K. A. Robbins, Periodic Solutions and Bifurcation Structure at High R in the Lorenz Model, *SIAM J. Appl. Math.* **36**:457 (1979).